Completing a Charge Transport Chain for Artificial Photosynthesis

Journal:	*Journal of the American Chemical Society*
Manuscript ID	ja-2018-06740w
Manuscript Type:	Communication
Date Submitted by the Author:	26-Jun-2018
Complete List of Authors:	Eberhart, Michael; University of North Carolina at Chapel Hill, Department of Chemistry Bowers, Leah; University of North Carolina at Chapel Hill, Department of Chemistry Shan, Bing; University of North Carolina at Chapel Hill, Chemistry Troian-Gautier, Ludovic; University of North Carolina at Chapel Hill, Chemistry Brennaman, M.; U. North Carolina - Chapel Hill, Chemistry Papanikolas, John; University of North Carolina, Department of Chemistry Meyer, Thomas; University of North Carolina, Chemistry

Completing a Charge Transport Chain for Artificial Photosynthesis

Michael S. Eberhart, Leah M. Rader Bowers, Bing Shan, Ludovic Troian-Gautier, M. Kyle Brennaman, John M. Papanikolas, and Thomas J. Meyer*

Department of Chemistry, University of North Carolina at Chapel Hill, CB 3290, Chapel Hill, North Carolina 27599, United States

Supporting Information Placeholder

ABSTRACT: A ruthenium polypyridyl chromophore with electronically isolated triarylamine substituents has been synthesized which models the role of tyrosine in the electron transport chain in Photosystem II. When bound to the surface of a TiO_2 electrode, electron injection from a Ru(II) Metal-to-Ligand Charge Transfer (MLCT) excited state occurs from the complex to the electrode to give Ru(III). Subsequent rapid electron transfer from the pendant triarylamine to Ru(III) occurs with an observed rate constant of ~10^{10} s^{-1} which is limited by the rate of electron injection into the semiconductor. Transfer of the oxidative equivalent away from the semiconductor surface results in dramatically reduced rates of back electron transfer, and a long lived (τ = ~0.5 ms) triarylamine radical cation that is used to oxidize hydroquinone in solution.

In photosystem II, chlorophyll P680 is excited followed by the transfer of electrons through a series of redox intermediates to give a reduced quinone and oxidized tyrosine. The electrons are eventually transferred to Photosystem I where they are used in the production of NADPH while the oxidized tyrosine is the oxidant that activates the oxygen evolving complex (OEC).[1] The electron transport chain consists of a series of redox couples that spatially separate charges generated by light absorption with minimal energy loss with charge separated lifetimes that are sufficiently long to accommodate relatively slow water oxidation at the OEC.

In the electron transport chain in photosystem II, electron transfer occurs from tyrosine Z (Y_z) to oxidized chlorophyll P680. There is evidence that suggests that the oxidation of Y_z is coupled to proton transfer.[2–5] Oxidation of Y_z, with concurrent proton transfer to the base His190, creates a transiently stabilized redox intermediate that is sufficiently long-lived to activate the OEC through a complete $4e^-/4H^+$ water oxidative cycle.[6,7] Y_z plays its role as a redox shuttle by absorbing oxidative equivalents on a transient basis from $P680^{\bullet+}$, avoiding decomposition of the radical cation.

The role that Y_z plays in the stepwise oxidation of water at the OEC may also be important for water oxidation at photoanodes in artificial photosynthesis. Although there is precedence for phenols serving as traps for oxidative equivalents,[8–13] and a phenol-based trap has been shown to enhance water oxidation,[14,15] the magnitudes of their redox potentials and a lack of aqueous stabilities have, so far, limited their usefulness for water oxidizing photoanodes. Balancing the thermodynamics in a process involving both electrons and protons for artificial photosynthesis remains a formidable challenge.

An alternative to phenols are triarylamine (Ar_3N) donors. They offer well-defined $Ar_3N^{\bullet+/0}$ couples and relatively well-understood electrochemistry in non-aqueous solvents.[16–27] In the family of Ar_3N donors, there is a systematic basis for modulating redox potentials allowing them to overlap with the requirements for activating water oxidation catalysis,[16–19,25–27] although there are only limited results in aqueous solutions.[28] Barriers to electron transfer are also low; bis-triarylamines have been used to demonstrate fast intervalence charge-transfer with rates that imply that electron transfer self-exchange rates in solution for Ar_3N species should be diffusion limited.[29] Triarylamines are colorless and not parasitic light absorbers. Upon oxidation, triarylamine radical cations have distinct spectral features in the low energy visible that provides a useful spectroscopic probe of electron transfer.[30,31]

There are reports of Ru(II) polypyridyl complexes with pendant donors. Bignozzi and G. Meyer showed that Ru(II) polypyridyl photosensitizers with phenothiazine substituents improved charge separated lifetimes.[32] A chromophore featuring both triarylamine donors and an anthraquinone acceptor has been shown to result in a transient charge-transfer state with a lifetime of 870 ns following MLCT excitation.[33] Surface-bound ruthenium dyes linked to $Ar_2Ar'N$ groups through an unsaturated bridge have exhibited electron recombination lifetimes from 350 μs to 5 ms depending on the nature of the $Ar_2Ar'N$ derivatives.[34] Light absorption by another Ru(II) chromophore, bound to an extended oligomer of ~100 TPA units linked by a saturated backbone, leads to a very long-lived redox-separated state with a lifetime of 4 s.[34] Species containing multiple amine substituents have been used to show that multiple oxidative equivalents can be accumulated at a common site.[35,36] Reports have also appeared that investigate the role of thermodynamics, kinetics and photophysics on electron transfer reactions between surface-bound Ru^{3+} and triarylamines in solution and on surfaces.[25,31,37]

With the goal of utilizing triarylamines for the transient storage of oxidative equivalents in photo-induced electron transfer reactions in water oxidation, we have initiated a systematic investigation of the Ru(II) polypyridyl complex $\mathbf{P_2RuTPA^{2+}}$ shown in Figure 2 and its analog that lacks phosphonic esters, $\mathbf{RuTPA^{2+}}$.In these experiments, we have sensitized electrodes using phosphonate esters rather than the corresponding phosphonic acids for solubility reasons. Phosphonic esters are known to form stable surface bonds to metal oxides and the mode of binding to the surface may not involve hydrolysis to the corresponding phosphonic acid.[38]

The electrochemical properties of $\mathbf{RuTPA^{2+}}$ were investigated by cyclic voltammetry in acetonitrile containing 0.1 M [nBu$_4$N][PF$_6$] as electrolyte. Reversible waves were observed at $E_{1/2}$ = 0.46 and 0.89 V vs $Fc^{+/0}$, for the $Ar_2Ar'N^{+\bullet/0}$ and $Ru^{3+/2+}$ couples, respectively (Figure S1). A broad, irreversible wave at 0.75 V vs $Fc^{+/0}$ was also observed for the $Ar_2Ar'N^{2+/+\bullet}$ couple (Figure S1).

Peak currents for the $Ar_2Ar'N^{+\bullet/0}$ wave were twice that for the $Ru^{3+/2+}$couple, consistent with oxidation of the triarylamines at a single potential separated by a statistical factor demonstrating that they are electronically isolated.

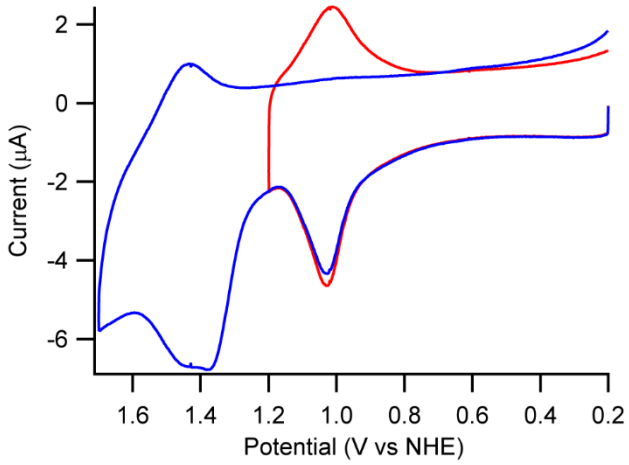

Figure 1. Cyclic voltammograms of **P_2RuTPA^{2+}** adsorbed on FTO glass in 0.1M HBF_4. (Red) First scan to 1.2 V vs NHE. (Blue) Second scan to 1.7 V vs NHE.

Aqueous surface electrochemistry was explored by adsorbing **P_2RuTPA^{2+}** on conductive, FTO glass electrode surfaces. Under aqueous conditions (0.1 M HBF_4), the $Ar_2Ar'N^{+\bullet/0}$ wave is reversible with $E_{1/2}$ = 1.02 V vs NHE (Figure 1, red trace). Scanning to more positive potentials provides evidence for additional waves (Figure 1, blue trace). A second, irreversible, oxidation of $Ar_2Ar'N$ is observed at $E_{p,a}$ = 1.38 V vs NHE with a reversible $Ru^{3+/2+}$ wave with $E_{1/2}$ = 1.46 V vs NHE (Figure 1, blue trace). After scanning past the $Ar_2Ar'N^{2+/+\bullet}$ wave, reduction of $Ar_2Ar'N^{+\bullet}$ to $Ar_2Ar'N^0$ is no longer observed, pointing to irreversible oxidation of the triarylamine donor. In order for the $Ar_2Ar'N$ groups to function effectively as part of photoanodes for water oxidation, the $Ar_2Ar'N^{+\bullet/0}$ couple should provide sufficient driving force to activate a water oxidation catalyst and be kinetically capable of reducing an oxidized photosensisitizer.

When bound to a mesoporous, nanoparticle TiO_2 semiconductor electrode (4 μm, 15 nm particles) and excited with visible light, **P_2RuTPA^{2+}** undergoes a series of electron transfer reactions. The reactions are summarized in eq 1-3 and illustrated in Figure 2. In the initial step, the MLCT chromophore is excited (eq 1) and an electron is injected into TiO_2 (eq 2). Injection gives the oxidized form of the complex, Ru(III). Rapid reduction of Ru(III) to Ru(II) follows with transfer of an oxidative equivalent to an external $Ar_2Ar'N$ amine (eq 3). The sequence of electron transfer reactions is shown by the half arrows in Figure 2.

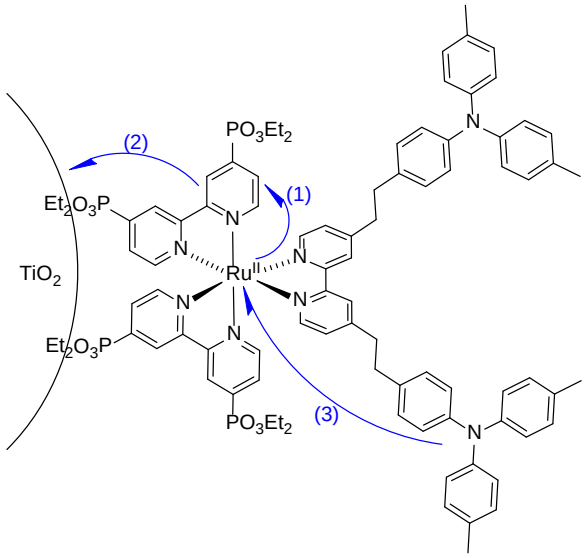

Figure 2. **P_2RuTPA^{2+}** bound to a TiO_2 semiconductor. The blue half-arrows illustrate the electron transfer reactions in eq 1, 2, and 3.

$$TiO_2\,|\,[P_2Ru^{II}TPA]^{2+} \xrightarrow{h\nu} TiO_2\,|\,[P_2Ru^{II}TPA]^{2+*} \quad (1)$$

$$TiO_2\,|\,[P_2Ru^{II}TPA]^{2+*} \longrightarrow TiO_2(e^-)\,|\,[P_2Ru^{III}TPA]^{3+} \quad (2)$$

$$TiO_2(e^-)\,|\,[P_2Ru^{III}TPA]^{3+} \longrightarrow TiO_2(e^-)\,|\,[P_2Ru^{II}TPA^{+\bullet}]^{3+} \quad (3)$$

Electron injection from the excited state into TiO_2 occurs on the picosecond time scale and is followed by electron transfer from a pendant $Ar_2Ar'N$ to Ru(III). Electron injection occurs with a rate constant of k = 1.2(3) x 10^{10} s^{-1}, based on single exponential fits to absorption-time traces at 385 nm (Figure S2). The rate of injection is similar to rates observed for related Ru(II) chromophores that lack the $Ar_2Ar'N$ substituents.[39–41] However, for molecules on TiO_2 without the $Ar_2Ar'N$ substituents, the MLCT bleach persists for microseconds with back electron transfer to Ru(III) occurring on the microsecond timescale. For **P_2RuTPA^{2+}**, recovery of the bleach is rapid with injection followed by electron transfer to Ru(III) from a pendant $Ar_2Ar'N$ group. Electron transfer from $Ar_2Ar'N$ to Ru(III) can be monitored by recovery of the ground state bleach at 450 nm and by the appearance of the $Ar_2Ar'N^{\bullet+}$ radical cation at 690 nm. The first-order kinetics observed with rate constants of 1.1(2) x 10^{10} s^{-1} at 450 nm and 9(1) × 10^9 s^{-1} at 690 nm are consistent with rate-limiting electron injection followed by rapid intra-assembly electron transfer.

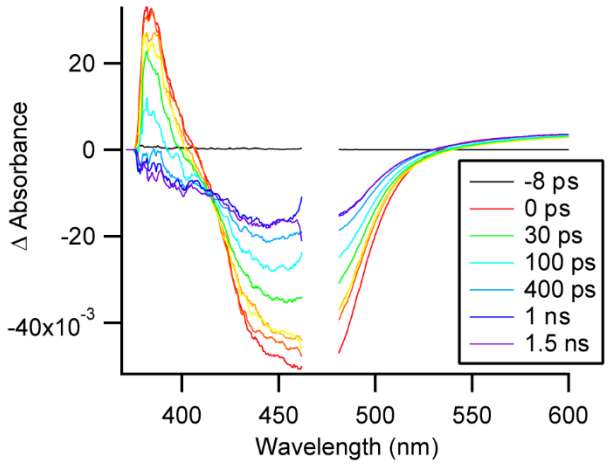

Figure 3. Transient absorption spectral changes between 0 (red) and 1.5 ns (purple) after pulsed 470 nm excitation (120 nJ/pulse) of $\mathbf{P_2RuTPA^{2+}}$ on TiO_2 in argon purged, aqueous 0.1 M HBF_4.

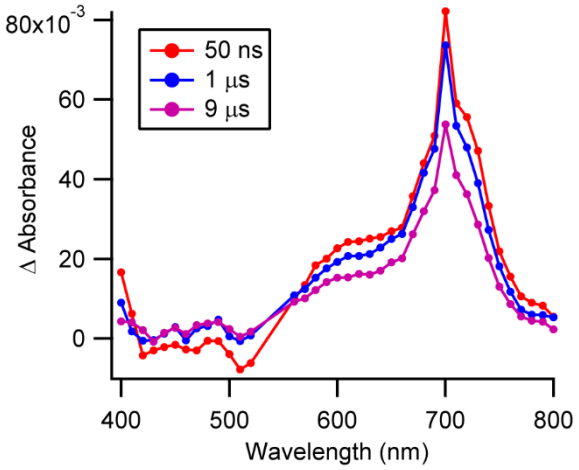

Figure 4. Nanosecond transient absorption spectra showing oxidized $Ar_2Ar'N^{+\bullet}$ in $\mathbf{P_2RuTPA^{2+}}$ on TiO_2 in 0.1 M HBF_4 (aqueous) following pulsed 532 nm laser excitation (2 mJ/pulse).

On the nanosecond time scale, an absorption at λ_{max} at 700 nm appeared immediately following excitation of $\mathbf{P_2RuTPA^{2+}}$ consistent with appearance of the radical cation $Ar_2Ar'N^{+\bullet}$, Figure 4. The lifetime of the transient, $TiO_2(e^-)$|-[$\mathbf{P_2Ru^{II}TPA^{+\bullet}}$]$^{3+}$, was ~0.5 ms demonstrating that spatially removing the oxidative equivalent from the electrode dramatically reduces the rate of back electron transfer.

Electron transfer from $Ar_2Ar'N$ to Ru^{3+} following visible excitation of $\mathbf{P_2RuTPA^{2+}}$ occurred with high efficiency. With an incident photon flux of ~18 nmol/cm^2, determined by actinometry with $Ru(bpy)_3^{2+}$ in acetonitrile as the actinometer, the internal quantum efficiency for formation of $TiO_2(e^-)$|-[$\mathbf{P_2Ru^{II}TPA^{+\bullet}}$]$^{3+}$ based on absorbance at 50 ns time delay was ~60%.

Photoexcitation of $\mathbf{P_2RuTPA^{2+}}$ was also explored on ZrO_2 (Figure 5). ZrO_2 films provide a chemical environment similar to TiO_2 but without electron transfer to or from the electrode. Analysis of the emission spectrum of $\mathbf{P_2RuTPA^{2+*}}$ by single-mode Franck-Condon line shape analysis (Figure S7) in 0.1 M aqueous HBF_4 gave 2.12 eV for the free energy of the excited-state above the ground state. Based on the excited-state energy and E^0 = -1.82 V vs $Fc^{+/0}$ (~ -1.18 V vs NHE) for the $\mathbf{P_2RuTPA^{2+/+}}$ couple in acetonitrile, E^0 is 0.94 V vs NHE for the $\mathbf{P_2RuTPA^{2+/+*}}$ excited-state couple. Based on this value, the potential difference between the $\mathbf{P_2RuTPA^{2+*/+}}$ and $\mathbf{Ar_2Ar'N^{+\bullet/0}}$ couples is relatively small. The results of transient nanosecond flash photolysis measurements in Figure 5 provide evidence that following nanosecond excitation of $\mathbf{P_2RuTPA^{2+}}$ on ZrO_2, both of the states, [$\mathbf{PP^-Ru^{III}TPA}$]$^{2+}$ and [$\mathbf{PP^{-\bullet}Ru^{II}TPA^{+\bullet}}$]$^{2+}$, exist on the electrode surface.

Figure 5 illustrates the results of a flash photolysis experiment following 10 ns, 532 nm flash excitation of the complex on ZrO_2 in aqueous 0.1 M HBF_4. In the transient spectrum, there is clear evidence for the MLCT excited state, |-$\mathbf{[PP^-Ru^{III}TPA]^{2+}}$, by the MLCT transient bleach feature at 460 nm. There is also evidence for the intra-assembly electron transfer intermediate |-$\mathbf{[PP^{-\bullet}Ru^{II}TPA^{+\bullet}]^{2+}}$, by the positive absorption feature at 700 nm, eq 4. Based on relative molar extinction coefficients at 475 nm for the bleach, and at 700 nm for the cation radical, the ratio of $\mathbf{[PP^{-\bullet}Ru^{II}TPA^{+\bullet}]^{2+}}$ to $\mathbf{[PP^{-\bullet}Ru^{III}TPA]^{2+}}$, was ~1:4 after 20 ns with luminescence also observed for ZrO_2|-[$PP^-Ru^{III}TPA$]$^{2+*}$. The weighted average lifetime for decay of biexponential kinetic fits of the ground state bleach at 460 nm for ZrO_2|-[$PP^-Ru^{III}TPA$]$^{2+}$ was 125 ns and for decay of the amine-based state, ZrO_2|-[$PP^-Ru^{II}TPA^{+\bullet}$]$^{2+}$, 437 ns.

ZrO_2|-[$\mathbf{P_2Ru^{II}TPA}$]$^{2+}$ hν → ZrO_2|-[$\mathbf{P_2Ru^{II}TPA}$]$^{2+*}$ →

ZrO_2|-[$\mathbf{PP^{-\bullet}Ru^{III}TPA^{+\bullet}}$]$^{2+*}$ (~20%) +

ZrO_2|-[$\mathbf{PP^{-\bullet}Ru^{III}TPA}$]$^{2+}$ (~80%) (4)

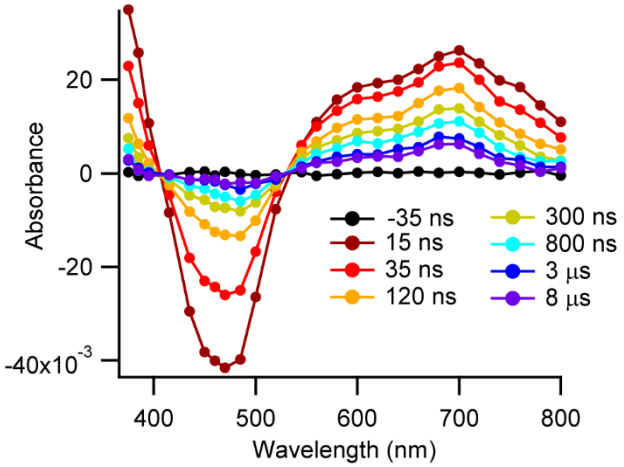

Figure 5. Transient absorption difference spectra for $\mathbf{P_2RuTPA^{2+}}$ on ZrO_2 in aqueous 0.1 M HBF_4.

As a proof of the transient redox storage concept, oxidative equivalents stored on the $Ar_2Ar'N^{+\bullet}$ groups on TiO_2 were also shown to oxidize hydroquinone dissolved in the external electrolyte. When $\mathbf{P_2RuTPA^{2+}}$ was loaded on mesoporous FTO|TiO_2 electrodes, photocurrents of ~500 μA•cm^{-2} were obtained under 1 sun illumination in aqueous 0.1 M HBF_4 solutions containing 60 mM hydroquinone (Figure 6). The photocurrent was sustained at the ~500 μA•cm^{-2} level for one hour.

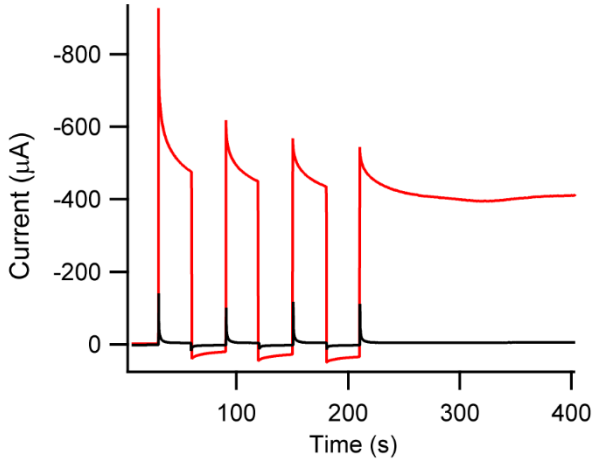

Figure 6. (red)Photocurrents for FTO||TiO_2| **P_2RuTPA^{2+}** in 0.1 M HBF_4 containing 60 mM hydroquinone and without hydroquinone, (black).

The new ruthenium(II) polypyridyl dyes, with electronically isolated triarylamines, offer a well-defined molecular geometry and a well-defined stoichiometric relationship between the amines and the ruthenium complex. Their greatly decreased back electron transfer timescales, following excitation and intra-assembly electron transfer, may assist in the catalysis of multiple electron transfer reactions such as water oxidation. In these schemes, rapid reduction of Ru(III) to Ru(II) may also enhance catalyst lifetimes by minimizing the time spent as Ru(III), avoiding catalyst instability at the higher oxidation state in electrode applications.[43]

ASSOCIATED CONTENT

Supporting Information

The Supporting Information is available free of charge on the ACS Publications website. Compound synthesis and characterization data, experimental details of transient absorption experiments, electrode, kinetics analysis, and additional electrochemical and spectroscopic data are included in supporting information (PDF).

AUTHOR INFORMATION

Corresponding Author

*tjmeyer@unc.edu

ORCID

Michael S. Eberhart: 0000-0002-6261-5727
Ludovic Troian-Gautier: 0000-0002-7690-1361
John M. Papanikolas: 0000-0002-0902-6990
Thomas J. Meyer: 0000-0002-7006-2608

Notes

The authors declare no competing financial interests.

ACKNOWLEDGMENT

This research was solely supported by the UNC EFRC Center for Solar Fuels, an Energy Frontier Research Center funded by the U.S. Department of Energy, Office of Science, Office of Basic Energy Sciences under Award Number DE-SC0001011.

REFERENCES

(1) Ferreira, K. N.; Iverson, T. M.; Maghlaoui, K.; Barber, J.; Iwata, S. *Science (80-.).* **2004**, *303*, 1831–1838.
(2) Meyer, T. J.; Huynh, M. H. V.; Thorp, H. H. *Angew. Chemie Int. Ed.* **2007**, *46*, 5284–5304.
(3) Migliore, A.; Polizzi, N. F.; Therien, M. J.; Beratan, D. N. *Chem. Rev.* **2014**, *114*, 3381–3465.
(4) Weinberg, D. R.; Gagliardi, C. J.; Hull, J. F.; Murphy, C. F.; Kent, C. A.; Westlake, B. C.; Paul, A.; Ess, D. H.; McCafferty, D. G.; Meyer, T. J. *Chem. Rev.* **2012**, *112*, 4016–4093.
(5) Kühne, H.; Brudvig, G. W. *J. Phys. Chem. B* **2002**, *106*, 8189–8196.
(6) Kok, B.; Forbush, B.; McGloin, M. *Photochem. Photobiol.* **1970**, *11*, 457–475.
(7) Vinyard, D. J.; Ananyev, G. M.; Dismukes, G. C. *Annu. Rev. Biochem.* **2013**, *82*, 577–606.
(8) Altwicker, E. R. *Chem. Rev.* **1967**, *67*, 475–531.
(9) Manbeck, G. F.; Fujita, E.; Concepcion, J. J. *J. Am. Chem. Soc.* **2016**, *138*, 11536–11549.
(10) Irebo, T.; Zhang, M.-T.; Markle, T. F.; Scott, A. M.; Hammarström, L. *J. Am. Chem. Soc.* **2012**, *134*, 16247–16254.
(11) Zhang, M.-T.; Irebo, T.; Johansson, O.; Hammarström, L. *J. Am. Chem. Soc.* **2011**, *133*, 13224–13227.
(12) Megiatto Jr, J. D.; Méndez-Hernández, D. D.; Tejeda-Ferrari, M. E.; Teillout, A.-L.; Llansola-Portolés, M. J.; Kodis, G.; Poluektov, O. G.; Rajh, T.; Mujica, V.; Groy, T. L.; et al. *Nat Chem* **2014**, *6*, 423–428.
(13) Concepcion, J. J.; Brennaman, M. K.; Deyton, J. R.; Lebedeva, N. V; Forbes, M. D. E.; Papanikolas, J. M.; Meyer, T. J. *J. Am. Chem. Soc.* **2007**, *129*, 6968–6969.
(14) Youngblood, W. J.; Lee, S.-H. A.; Kobayashi, Y.; Hernandez-Pagan, E. A.; Hoertz, P. G.; Moore, T. A.; Moore, A. L.; Gust, D.; Mallouk, T. E. *J. Am. Chem. Soc.* **2009**, *131*, 926–927.
(15) Zhao, Y.; Swierk, J. R.; Megiatto, J. D.; Sherman, B.; Youngblood, W. J.; Qin, D.; Lentz, D. M.; Moore, A. L.; Moore, T. A.; Gust, D.; et al. *Proc. Natl. Acad. Sci.* **2012**, *109*, 15612–15616.
(16) Seo, E. T.; Nelson, R. F.; Fritsch, J. M.; Marcoux, L. S.; Leedy, D. W.; Adams, R. N. *J. Am. Chem. Soc.* **1966**, *88*, 3498–3503.
(17) Nelson, R. R.; Adams, R. N. *J. Am. Chem. Soc.* **1968**, *90*, 3925–3930.
(18) Bender, T. P.; Graham, J. F.; Duff, J. M. *Chem. Mater.* **2001**, *13*, 4105–4111.
(19) Dapperheld, S.; Steckhan, E.; Brinkhaus, K.-H. G.; Esch, T. *Chem. Ber.* **1991**, *124*, 2557–2567.
(20) Larumbe, D.; Gallardo, I.; Andrieux, C. P. *J. Electroanal. Chem. Interfacial Electrochem.* **1991**, *304*, 241–247.
(21) Wain, A. J.; Streeter, I.; Thompson, M.; Fietkau, N.; Drouin, L.; Fairbanks, A. J.; Compton, R. G. *J. Phys. Chem. B* **2006**, *110*, 2681–2691.
(22) Steckhan, E. *Angew. Chemie Int. Ed. English* **1986**, *25*, 683–701.
(23) Adams, R. N. *Acc. Chem. Res.* **1969**, *2*, 175–180.
(24) Nelson, R. F.; Philp, R. H. *J. Phys. Chem.* **1979**, *83*, 713–716.
(25) DiMarco, B. N.; Troian-Gautier, L.; Sampaio, R. N.; Meyer, G. J. *Chem. Sci.* **2018**, *9*, 940–949.
(26) Schmidt, W.; Steckhan, E. *Chem. Ber.* **1980**, *113*, 577–585.
(27) Steckhan, E. In *Topics in Current Chemistry*; Berlin, 1987; Vol. 142, pp 1–69.
(28) Eberhart, M. S.; Wang, D.; Sampaio, R. N.; Marquard, S. L.; Shan, B.; Brennaman, M. K.; Meyer, G. J.; Dares, C.; Meyer, T. J. *J. Am. Chem. Soc.* **2017**, *139*, 16248–16255.
(29) Lambert, C.; Nöll, G. *J. Am. Chem. Soc.* **1999**, *121*, 8434–8442.
(30) Amthor, S.; Noller, B.; Lambert, C. *Chem. Phys.* **2005**, *316*, 141–152.
(31) Troian-Gautier, L.; DiMarco, B. N.; Sampaio, R. N.; Marquard, S. L.; Meyer, G. J. *J. Am. Chem. Soc.* **2018**, *140*, 3019–3029.
(32) Argazzi, R.; Bignozzi, C. A.; Heimer, T. A.; Castellano, F. N.; Meyer, G. J. *J. Am. Chem. Soc.* **1995**, *117*, 11815–11816.
(33) Orazietti, M.; Kuss-Petermann, M.; Hamm, P.; Wenger, O. S. *Angew. Chemie Int. Ed.* **2016**, *55*, 9407–9410.
(34) Haque, S. A.; Handa, S.; Peter, K.; Palomares, E.; Thelakkat, M.; Durrant, J. R. *Angew. Chemie Int. Ed.* **2005**, *44*, 5740–5744.
(35) Karlsson, S.; Boixel, J.; Pellegrin, Y.; Blart, E.; Becker, H.-C.; Odobel, F.; Hammarström, L. *J. Am. Chem. Soc.* **2010**, *132*,

17977–17979.
(36) Chen, H.-Y.; Ardo, S. *Nat. Chem.* **2017**, *10*, 17.
(37) Hu, K.; Blair, A. D.; Piechota, E. J.; Schauer, P. A.; Sampaio, R. N.; Parlane, F. G. L.; Meyer, G. J.; Berlinguette, C. P. *Nat. Chem.* **2016**, *8*, 853.
(38) Guerrero, G.; Mutin, P. H.; Vioux, A. *Chem. Mater.* **2001**, *13*, 4367–4373.
(39) Gish, M. K.; Lapides, A. M.; Brennaman, M. K.; Templeton, J. L.; Meyer, T. J.; Papanikolas, J. M. *J. Phys. Chem. Lett.* **2016**, *7*, 5297–5301.
(40) Swierk, J. R.; McCool, N. S.; Nemes, C. T.; Mallouk, T. E.; Schmuttenmaer, C. A. *J. Phys. Chem. C* **2016**, *120*, 5940–5948.
(41) Zigler, D. F.; Morseth, Z. A.; Wang, L.; Ashford, D. L.; Brennaman, M. K.; Grumstrup, E. M.; Brigham, E. C.; Gish, M. K.; Dillon, R. J.; Alibabaei, L.; et al. *J. Am. Chem. Soc.* **2016**, *138*, 4426–4438.
(42) Gould, I. R.; Ege, D.; Moser, J. E.; Farid, S. *J. Am. Chem. Soc.* **1990**, *112*, 4290–4301.
(43) Hyde, J. T.; Hanson, K.; Vannucci, A. K.; Lapides, A. M.; Alibabaei, L.; Norris, M. R.; Meyer, T. J.; Harrison, D. P. *ACS Appl. Mater. Interfaces* **2015**, *7*, 9554–9562.